Effects of medium fluid cavitation on fluctuation characteristics of magnetic fluid seal interface in agricultural centrifugal pump

Zhenggui Li[1*], Wangxu Li[1], Qifan Wang[2], Ru Xiang[1], Jie Cheng[1], Wei Han[3], Zhaoqiang Yan[4]

(1. *Key Laboratory of Fluid and Power Machinery, Ministry of Education, Xihua University, Chengdu 610039, China*;
2. *Huaneng Gansu Hydropower Development Co., Ltd, Lanzhou 730000, China*;
3. *School of Energy and Power Engineering, Lanzhou University of Technology, Lanzhou 730050, China*;
4. *Zigong Zhaoqiang Sealing Products Industrial Co., Ltd, Zigong 643000, Sichuan, China*)

Abstract: The fluctuation law of magnetic fluid seal interface of an agricultural centrifugal pump is theoretically unknown; the pressure and velocity fluctuations are crucial factors that cause interface fluctuation. In this study, the pressure and velocity fluctuations of the sealing interface on an agricultural centrifugal pump during cavitation were investigated based on the methods of Ansys CFX numerical calculation and experimental verification. The results demonstrated that at the same flow rate, the pressure fluctuation amplitude of the sealing interface decreased gradually from the shaft surface to the bottom of the polar tooth. At different flow rates, the amplitude of the pressure fluctuation decreased with an increase in the flow rate. The cavitation of the medium aggravated the impact and water hammer of the liquid, leading to the occurrence of the jitter phenomenon in the sealing interface to accelerate the fluctuation frequency of the axial velocity of the sealing liquid, which accelerated the emulsification of the magnetic fluid. This law can provide a reference for the design of magnetic fluid sealing devices for agricultural centrifugal pumps.

Keywords: centrifugal pump, magnetic liquid sealing device, medium cavitation, interface fluctuations
DOI: 10.25165/j.ijabe.20211406.6718

Citation: Li Z G, Li W X, Wang Q F, Xiang R, Cheng J, Han W, et al. Effects of medium fluid cavitation on fluctuation characteristics of magnetic fluid seal interface in agricultural centrifugal pump. Int J Agric & Biol Eng, 2021; 14(6): 85–92.

1 Introduction

Centrifugal pump is a common agricultural hydraulic machinery, whose working principle is to convert the mechanical energy of the prime mover into liquid energy[1]. The traditional sealing method of a centrifugal pump is contact sealing; however, it has limitations, such as high friction and easy wearability[2], which causes short circuit in the prime mover and burning of associated equipment owing to leakage and failure of the seal. Therefore, a new type of seal is urgently required to replace the traditional seal. Recently developed magnetic fluid seals have the advantages of zero leakage, easy maintenance, low friction, and high reliability[3-5], thereby offering superior sealing conditions in centrifugal pumps[6].

Stability of a sealing interface is the key to effective sealing of a magnetic liquid. In 1984, Japanese scholar Fukayama Shinichi proposed the immiscibility and interface stability of magnetic fluid and sealing fluid[7]. When the magnetic liquid is sealed, the fluid state of the sealing liquid is unstable, causing emulsion and dilution of the magnetic liquid at the interface, which subsequently causes sealing failure. To explore the interface stability mechanism of the magnetic fluid, several studies have been conducted on magnetic fluid sealing. Liu et al.[8] assumed that magnetic flux leakage is one of the reasons for interface instability and optimized the structure of the magnetic fluid sealing device. Superconducting magnetic sleeves and outer aluminum sleeves were added to the shaft and pole shoe, respectively, to reduce the device magnetic flux leakage. Qian et al.[9] studied the liquid velocity distribution of the sealing medium by deducing the theoretical formula, considering that relative motion is the key to destroying the stability of the interface. Szczęch[10] studied the interface instability caused by Kelvin Helmholtz instability, and reported that vortex is one of the reasons for seal instability. Wang[11] proposed that the shear stress on the interface surface has a significant influence on the stability of the interface in dynamic sealing; hence, the baffle structure was added to the original sealing structure to enhance the interface stability during rotary seal. Krakov et al.[12] determined the interface instability caused by the concentration difference between the magnetic liquid and non-magnetic liquid through theoretical calculations. Although the sealing liquid has been further developed with the joint efforts of scholars, the failure problem of sealing liquid has not been solved; therefore, the understanding of the failure mechanism of sealing liquid is not comprehensive.

The magnetic fluid sealing device comprises a permanent magnet, pole shoe, magnetic fluid, and rotating shaft[13]. Through the response characteristics of the magnetic fluid to a magnetic field[14], an O-shaped seal ring is formed at the sealing gap[15], using the magnetic field pressure difference at the location to produce sealing ability. Therefore, the position of the magnetic fluid at the bottom of the pole tooth corresponds to the pressure-bearing capacity. When the pressure of the sealing interface changed, the axial position of the magnetic fluid changed

Received date: 2021-04-27 **Accepted date**: 2021-10-23
Biographies: Wangxu Li, MS candidate, research interests: magnetic liquid sealing technology, application of PIV technology. Email: 1121076860@qq.com; **Qifan Wang**, MS candidate, research interests: cavitation characteristics of space fuel pump, Email: 1051692001@qq.com; **Ru Xiang**, MS candidate, research interests: pressure pulsation characteristics of disk pump, Email: 1411248914@qq.com; **Jie Cheng,** MS candidate, research interests: multiple physical field coupling, Email: 2213491305@qq.com; **Wei Han**, PhD, Professor, research interests: Internal flow characteristics of hydraulic machinery, Email: hanwei@lut.cn; **Zhaoqiang Yan**, MS candidate, research interests: magnetic liquid sealing, Email: 1204868635@qq.com
***Corresponding author: Zhenggui Li,** PhD, Professor, research interests: magnetic liquid sealing technology. Xihua University, Chengdu 610039, China. Tel: +86-17602832345, Email: lzhgui@mail.xhu.edu.cn.

accordingly (as shown in Figure 1). Meanwhile, the magnetic liquid is in direct contact with the sealing liquid at the bottom of the pole tooth, and the velocity fluctuation of the sealing fluid accelerates the emulsification and dilution of the magnetic fluid.

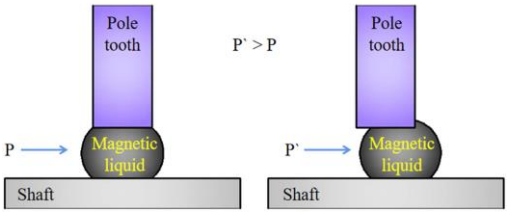

Figure 1 Interface fluctuation process of magnetoliquid seal

In the actual operation of an agricultural centrifugal pump, the flow field in the pump is complex[16-18]. Owing to the dynamic and static interference between the impeller and volute, the sealing interface produces larger pressure pulsation and velocity pulsation. The cavitation of the medium aggravates the fluctuation amplitude and adversely affects the interface stability of the magnetic fluid. In this study, the pressure fluctuation and velocity fluctuation of the sealing interface of the magnetic fluid sealing centrifugal pump shaft under the cavitation characteristics of the medium were studied using a combination of numerical calculation and experimental verification to provide a theoretical direction for a magnetic fluid-sealed centrifugal pump.

2 Materials and methods

When the centrifugal pump is in operation, most of the water flows to the volute through the centrifugal force, and flows out through the outlet. A small amount of water also flows into the shaft seal connected to the motor through the clearance channel, and is blocked by the magnetic fluid adsorbed on the bottom of the pole teeth (as shown in Figure 2). The flow process is considered a three-dimensional incompressible flow, and the flow field satisfies the mass conservation and momentum conservation equations.

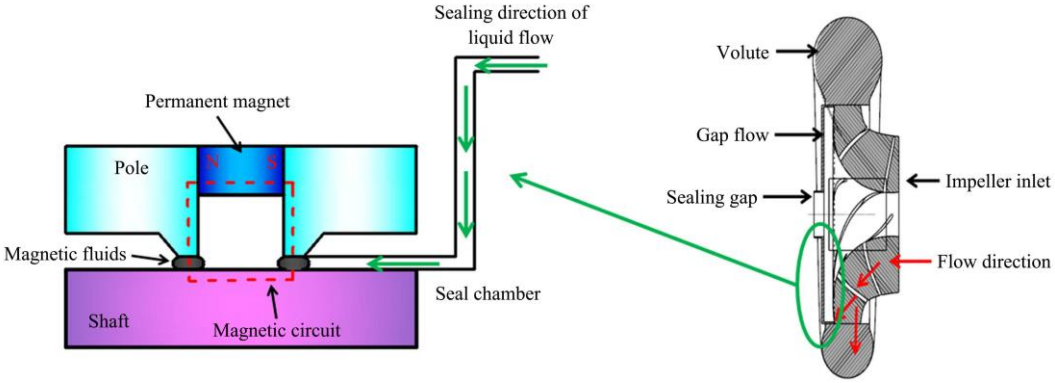

Figure 2 Schematic diagram of the model

In unit time (s), the fluid mass flowing out of the pump body is equal to the mass reduced by the density change in the pump body at the same time interval, that is, the conservation of fluid mass in the pump. The theoretical formula is as follows[19]:

$$\frac{\partial \rho}{\partial t}+\frac{\partial(\rho u_x)}{\partial x}+\frac{\partial(\rho u_y)}{\partial y}+\frac{\partial(\rho u_z)}{\partial z}=0 \tag{1}$$

During operation, the fluid in the pump is subjected to external forces, such as impact. The change rate of fluid momentum with respect to time is equal to the sum of various external forces acting on the fluid, that is, the conservation of fluid momentum in the pump. The theoretical formula is as follows[19]:

$$\rho\frac{du}{dt}=-\nabla P+\nabla\cdot[\tau]+\rho F \tag{2}$$

The flow in the pump is too complex, and the fluid presents a turbulent flow. Compared to the standard k-ε model, the RNG model has better precision and is more suitable for the calculation of rotating and swirl conditions. In this study, the k-ε RNG turbulence model in Ansys CFX was used to conduct numerical calculations for the centrifugal pump, and the turbulence equation is[20]:

$$\frac{\partial(\rho k u_i)}{\partial x_i}=\frac{\partial}{\partial x_j}[(u+\frac{u_t}{\sigma_k})\frac{\partial k}{\partial x_j}]+P_k-\rho\varepsilon \tag{3}$$

$$\frac{\partial(\rho\varepsilon\mu_i)}{\partial x_i}=\frac{\partial}{\partial x_j}[(u+\frac{u_t}{\sigma_\varepsilon})\frac{\partial \varepsilon}{\partial x_j}]+\frac{\varepsilon}{k}(c_1^*P_k-c_2\rho\varepsilon) \tag{4}$$

$$c_1^*=c_1-\frac{\eta(1-\frac{\eta}{\eta_0})}{1+\beta\eta^3} \tag{5}$$

$$\mu=(2E_{ij}\cdot E_{ij})^{1/2}\frac{k}{\varepsilon} \tag{6}$$

$$E_{ij}=\frac{1}{2}(\frac{\partial u_i}{\partial x_j}+\frac{\partial u_j}{\partial x_i}) \tag{7}$$

where, c_1=1.42, c_2=1.68, σ_k=0.72, σ_ε=0.75, and c_μ=0.0845.

The cavitation model is a calculation model that can solve the change in physical quantities between phases. In general, the Rayleigh-Plesset equation is used to describe the birth and collapse of cavitation[21]:

$$R_B\frac{d^2R_B}{dt^2}+\frac{3}{2}(\frac{dR_B}{dt})^2+\frac{4v}{R_B}\frac{dR_B}{dt}+\frac{2\sigma}{\rho_l R_B}=\frac{P_B-P}{\rho} \tag{8}$$

Assuming that there is no heat source and the terms of viscosity and surface tension are neglected, the equation can be simplified as follows:

$$\frac{dR_B}{dt}=\sqrt{\frac{2}{3}\frac{P_B-P}{\rho_l}} \tag{9}$$

In the calculation of the cavitation flow field, the vapor transport equation is used to control the gas-liquid mass transfer process, and the equation is shown as follows:

$$\frac{\partial}{\partial}(\alpha\rho_v)+\nabla(\alpha\rho_v u_v)=R_e-R_c \tag{10}$$

To study the pressure fluctuation and velocity fluctuation characteristics of the sealing interface in the process of cavitation of the centrifugal pump medium, unsteady flow calculations were performed under different flow rates of $0.8Q_r$, $1.0Q_r$, and $1.2Q_r$ (Q_r is the rated flow), and the pressure and velocity pulsations under the condition of non-cavitation and cavitation characteristics were

compared. Figure 3 shows the locations of the monitoring points at the sealing interface.

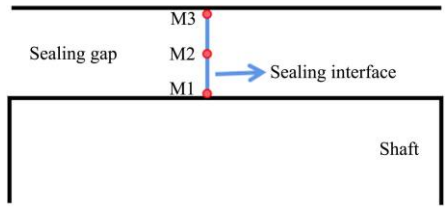

Figure 3 Location of monitoring points

The rated speed of the centrifugal pump, rated flow, shaft frequency, and blade frequency, were 2900 r/min, 100 m^3/h, 48.3 Hz, and 290 Hz, respectively, and the number of blades were six. The flow passage parts were the water inlet, impeller, volute, and seal clearance passages. The dynamic and static interfaces were connected by the transient rotor stator mode of the interface. The import was set to total pressure (stable), the exit was set to mass flow rate, and the cavitation model was Zwart-Gerber-Belamri. To ensure the accuracy of the numerical calculation, the inlet and outlet of the centrifugal pump were lengthened to ensure that the flow is fully developed and liquid backflow is inhibited, respectively. The seal clearance was 0.3 mm, the shaft surface at the clearance was a rotating wall, and the rotating speed was the rated speed. Because the actual shape of the sealing interface between the magnetic fluid and sealing fluid was difficult to survey owing to its complex nature, the sealing interface shape was idealized as a plane shape. The time step of the unsteady calculation was 1.7241×10^{-4} s, with 3 ° per revolution of impeller, 16 weeks in total calculation, and 0.33 s total time. After the calculation was stable, the results of the last four weeks were taken for analysis.

Owing to advantages such as small number of grids, high accuracy, and stable calculation, the numerical calculation adopted the structural grid drawn by ICEM CFD. Based on the verification of grid independence, the head of centrifugal pump was 20.1 m when the number of grids was 1528173, and 20.06 m when the number of grids was 1282918 at $0.8Q_r$. With an increase in the number of grids, the head change of the centrifugal pump was less than 3%, which was considered to meet the calculation requirements when the number of grids reached 1282918.

3 Results and discussion

3.1 Time domain analysis of pressure fluctuation at sealing interface during non-cavitation

Figure 4 shows the time domain diagram of the pressure fluctuation at different monitoring points without cavitation. To eliminate the influence of the static pressure of the monitoring point on the pressure fluctuation, the pressure was dimensionalized, and the pressure coefficient C_P was used to measure the pressure fluctuation[22].

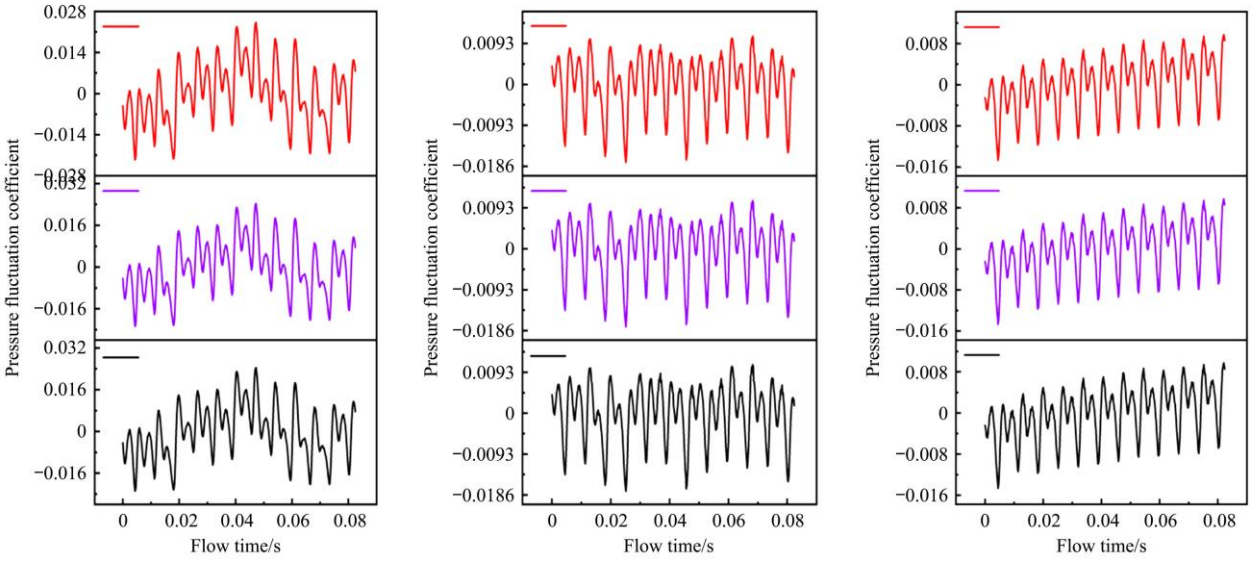

a. $0.8Q_r$ b. $1.0Q_r$ c. $1.2Q_r$

Figure 4 Time domain diagram of pressure pulsation (General)

Figure 4 shows a large pressure pulsation at the sealing interface of the centrifugal pump. At the same flow rate, the influence of the flow field in the pump on the pressure pulsation at the sealing interface was approximately the same owing to the small sealing clearance; therefore, the pressure pulsation trends at different monitoring points were similar. Table 1 lists the peak value of the pressure pulsation amplitude at the monitoring point without cavitation under different flow rates. Owing to the rotation of the main shaft, the surface of the shaft produced shear action on the sealing medium fluid, which caused fluid flow disorder, leading to pressure pulsation at the sealing interface. According to Newton's law of internal friction, the shear action decreases step-by-step along the radial direction. Therefore, the peak values of the sealing interface pressure fluctuation were the maximum at M1 point, and the peak value of M3 point was the minimum.

Table 1 Peak value of pressure pulsation amplitude without cavitation

	$0.8Q_r$	$1.0Q_r$	$1.2Q_r$
M1	221097	220113	219174
M2	203618	203538	203214
M3	201529	200555	199642

With the increase in flow rate, the fluid flow in the pump was fully developed, and the effect of flow disorder on pressure pulsation decreased; thus, the pressure pulsation at the sealing interface showed a trend of decreasing pulsation amplitude with the increase in flow rate. Moreover, several factors affected the pressure pulsation at the sealing interface; therefore, the periodicity of the pressure pulsation in the time domain diagram was weak.

The high and low pressures of the sealing interface led to the axial reciprocating motion of the magnetic fluid in the sealing gap. The frequency of the peak and trough of the pressure fluctuation determined the frequency of the axial reciprocating motion of the magnetic fluid. In four rotation cycles, there were 24 peaks and valleys at different monitoring points under different flow rates, indicating the existence of the same wave peaks and valleys in each rotation period as the number of blades. Therefore, in each rotation cycle, the magnetic fluid reciprocated six times, which is the same as the number of blades.

3.2 Time domain analysis of pressure fluctuation at seal interface during cavitation

Figure 5 shows the time domain diagram of the pressure fluctuation at different monitoring points during cavitation. It can be observed from Figure 5 that the amplitude of the pressure fluctuation at the sealing interface increased significantly after cavitation. The peak values of the pressure fluctuation amplitude at the monitoring points with cavitation under different flow rates are listed in Table 2. At $0.8Q_r$, $1.0Q_r$, and $1.2Q_r$, the peak value of the average pressure pulsation at three points (M1, M2 and M3) with cavitation were respectively 1.52, 1.53, and 1.52 times higher than that without cavitation. It can be seen that after cavitation, the axial distance of each position movement increased under the influence of pressure fluctuation. The variation in the pressure pulsation amplitude change law at the sealing interface was the same as that without cavitation, that is, the amplitude of the pressure pulsation from the main shaft along the radial direction to the bottom of the polar tooth, gradually decreased.

After cavitation, the fluid flow in the pump was disordered, the frequency of the peak and valley of the pressure fluctuation at the sealing interface had no obvious regularity, and several 'small peaks' existed between the two peaks. The small peaks caused vibrating of the sealing interface, which severely affected the sealing stability.

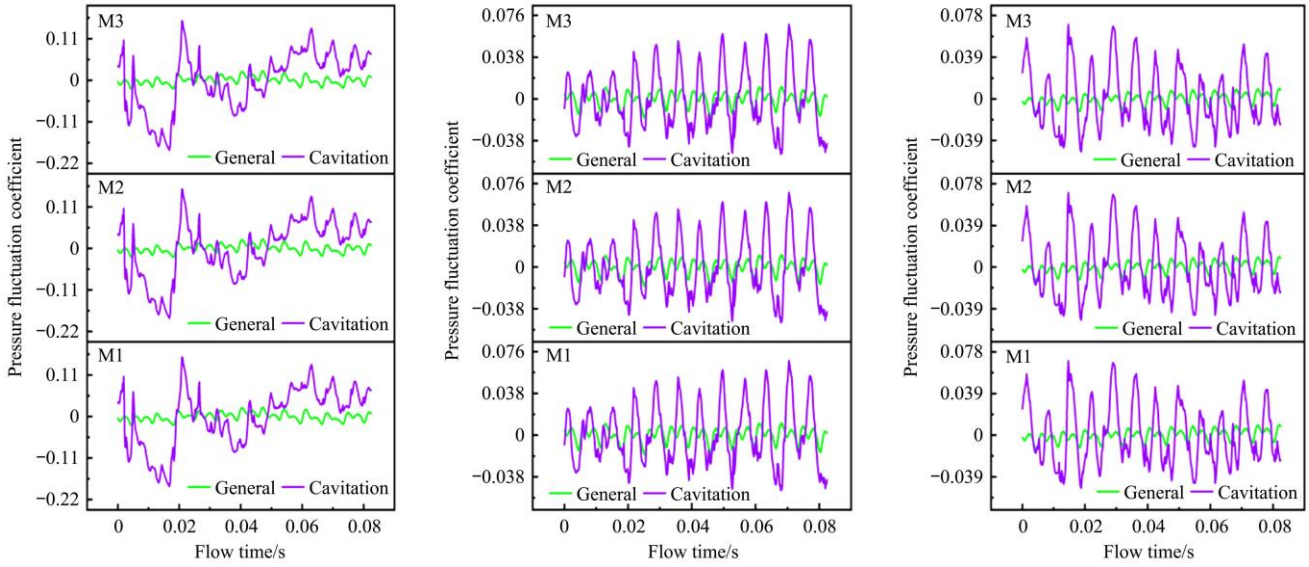

a. $0.8Q_r$ b. $1.0Q_r$ c. $1.2Q_r$

Figure 5 Time domain diagram of pressure pulsation (Cavitation)

Table 2 Peak value of pressure pulsation amplitude with cavitation

	$0.8Q_r$	$1.0Q_r$	$1.2Q_r$
M1	325366	324472	323229
M2	324408	315500	315554
M3	310229	309265	308336

3.3 Frequency domain analysis of pressure fluctuation at sealing interface during non-cavitation

To study the causes of pressure fluctuation at the sealing interface of the magnetic fluid in a centrifugal pump, the frequency domain diagram of pressure fluctuation at the sealing interface was obtained using the fast Fourier transform (FFT) of the fluid flow time and pressure fluctuation coefficient. The time domain information was lost; hence, the frequency domain information was accurately obtained by this method[23]. Because the pressure fluctuation trends of different monitoring points were similar during cavitation and non-cavitation, it can be seen that the causes of pressure fluctuation are the same. Therefore, only the M2 point was analyzed in the frequency domain analysis.

It can be observed from Figure 6 that at $0.8Q_r$, the pressure fluctuation at the sealing interface was mainly caused by the dynamic and static interference between the impeller and the volute, and the dominant frequency at that time was the leaf frequency. At $1.0Q_r$ and $1.2Q_r$, because of the increase in the inlet flow and velocity of the flow into the gap, the water flow in the gap impinged on the sealing interface, resulting in backflow and secondary impact owing to water hammer. Therefore, at $1.0Q_r$ and $1.2Q_r$, the main frequency shifted to the low frequency and appeared at 145 Hz. However, the dynamic and static interference between impeller and volute remained the key factor causing the pressure fluctuation at the seal interface. As a result, the secondary frequency appeared at the blade frequency. In addition to the dynamic and static interference, the disorder of the fluid flow pattern in the pump was the main factor causing pressure fluctuation at the sealing interface, which led to low-frequency signal. Therefore, with the increase in flow rate, the fluid flow in the pump was fully developed, the flow field was gradually stable, and the broadband pressure fluctuation at 0-145 Hz was gradually weakened. It can be observed that the dynamic and static interference between the impeller and the volute, fluid flow pattern in the pump cavity, backflow at the seal gap, and water hammer phenomenon are the main factors causing the pressure fluctuation at the magnetic fluid sealing interface.

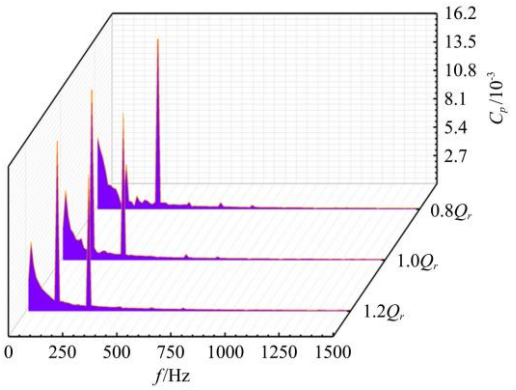

Figure 6 Frequency domain diagram of pressure fluctuation

3.4 Frequency domain analysis of pressure fluctuation of sealing interface under cavitation characteristics

As shown in Figure 7, when cavitation occurs in the pump, the main frequency of the pressure fluctuation of 0.8Q_r moves to a low frequency, and the main frequency of pressure pulsation at 1.0Q_r and 1.2Q_r shifts to high frequencies, both appearing at 145 Hz. This denotes that the main reason for the pressure fluctuation at the sealing interface is the flow disorder caused by cavitation. The secondary frequency is the blade frequency; therefore, the dynamic and static interference between the impeller and volute remained the key factor affecting the pressure fluctuation of the sealing interface.

In the range of 0-145 Hz exists the same law as that of non-cavitation, and the broadband pulsation gradually weakened with an increase in the flow rate. However, owing to the turbulence of the fluid in the pump cavity under cavitation characteristics, the impact of fluid in the sealing gap on the sealing interface was intensified, leading to an obvious increase in the broadband amplitude at low frequency compared with the frequency domain without cavitation at the same flow rate. Therefore, the occurrence of cavitation had a negative influence on the flow pattern of the sealing gap.

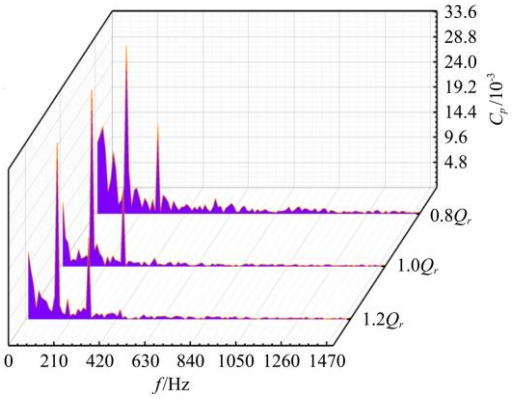

Figure 7 Frequency domain diagram of pressure pulsation under cavitation conditions

3.5 Velocity fluctuation analysis of sealing interface

The axial velocity fluctuation of the sealing fluid in the sealing cavity is an important factor in the mixing and emulsification of the magnetic fluid and sealing fluid. Therefore, the velocity fluctuation of the sealing interface was analyzed, as shown in Figure 8 (M1, M2, and M3 represent the three points during non-cavitation, and M10, M20, and M30 represent the three points during cavitation). When the flow rate increased, the fluid flow in the pump was fully developed, and the flow state became stable. Therefore, the axial velocity fluctuation at the sealing interface presented a phenomenon of decreasing amplitude with an increase in the flow rate. Cavitation had a negative impact on the stability of the flow field in the centrifugal pump; therefore, at the same flow rate, the axial velocity fluctuation frequency of the sealing interface was larger when cavitation occurred.

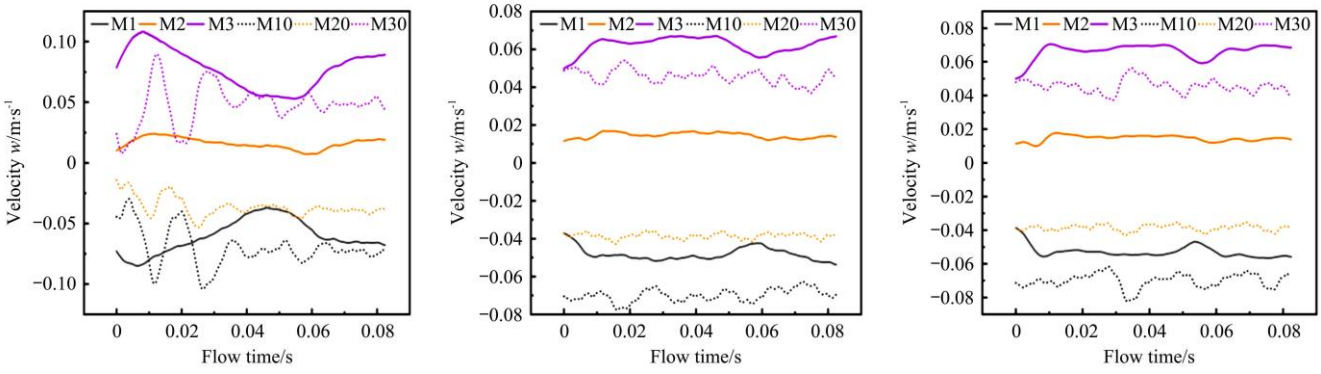

a. 0.8Q_r b. 1.0Q_r c. 1.2Q_r

Figure 8 Time domain diagram of velocity pulsation

In all flows, there were the following rules: the axial velocity of M3 was positive, that of M2 was 0, and that of M1 was negative. Furthermore, the velocity fluctuation at points M1 and M3 presented a symmetrical law regarding the M2 point, indicating that the fluid flowing into the sealing gap from the back of the blade has the greatest erosion effect on the magnetic fluid at the lower end of the pole tooth, and the erosion effect gradually decreased from the lower end of the pole tooth to the surface of the shaft. From the velocity distribution, it can be inferred that there is vortex movement in the sealing fluid near the sealing interface.

3.6 Flow field analysis at sealing gap

As shown in Figure 9, in the sealing cavity, the flow field is blocked by the magnetic fluid sealing interface, resulting in backflow. Furthermore, vortices are generated in the cavity, and the range of vortices decreases with an increase in the flow rate. The small bubbles generated by cavitation follow the liquid flowing from the sealing gap into the sealing cavity, and because of the existence of vortices in the cavity, they strike the sealing interface with the liquid to reduce the stability of the sealing interface.

Meanwhile, the pressure in the sealing cavity was slightly higher than the saturated vapor pressure of water at room temperature (20 ℃-25 ℃). When the small bubbles flowed into the sealing cavity with the liquid, they collapsed suddenly owing to the loss of existing conditions, and the liquid movement around the original small bubbles caused the local pressure to increase abruptly. When the small bubbles constantly formed in the liquid

flow and collapsed frequently near the sealing interface, the sealing interface was repeatedly impacted by huge pressure, causing interface fluctuation leading to sealing failure.

The volume fraction of small bubbles in the sealing cavity decreased with an increase in the flow rate, and the pressure fluctuation of the sealing interface caused by bubble collapse also decreased.

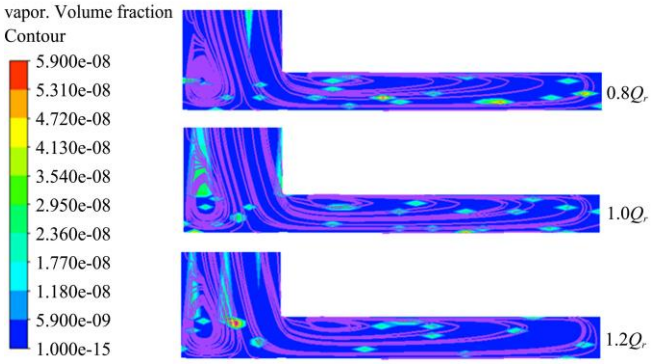

Figure 9 Flow field distribution in the sealed cavity

3.7 Test

To verify the accuracy of the numerical calculation, pressure pulsation tests of centrifugal pumps at 0.8, 1.0 and 1.2Q_r flow rates were performed at the Key Laboratory of Fluid and Power Machinery, Ministry of Education, Xihua University. The field device is illustrated in Figure 10. The test device was a circulation system, and the motor and centrifugal pump were connected through a torque sensor, which could measure the speed and torque of the motor in real time. The centrifugal pump supplied water through a tank located under the deck. The water flowed into the pump through the water inlet, and subsequently flowed into the water tank through the water outlet.

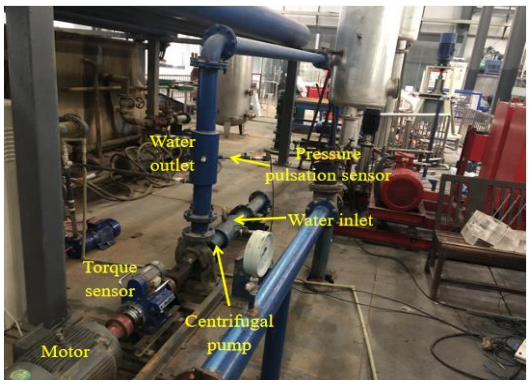

Figure 10 Schematic diagram of test device

The pump used in the test was a single-level single-suction high-speed horizontal centrifugal pump, and the specific parameters IS100-80-125 pump are listed in Table 3.

Table 3 Parameters of centrifugal pump

Parameters	Values
Inlet diameter of centrifugal pump/mm	100
Volute outlet diameter/mm	80
Shaft diameter of centrifugal pump/mm	56
Number of blades	6
Speed/r min^{-1}	2900
Head of delivery/m	20
Rated flow/m^3 h^{-1}	100
Shaft power/kW	7.0
Net positive suction head/m	4.5

In the test, a magnetic fluid sealing device was used to seal the shaft gap of the centrifugal pump, and the sealing gap was filled with excessive magnetic fluid. Figure 11 shows the magnetic fluid provided by the Key Laboratory of Fluid and Power Machinery, Ministry of Education, Xihua University, with oil as the base carrier, Fe_3O_4 as ferromagnetic particles, 0.036 T saturation magnetization, 1.35 g/cm^3 density, 34 mPa s viscosity, and −10 ℃-150 ℃ operating temperature. The running fluid in the pump was tap water at 25 ℃. During the operation of the pump, the heat generated by the viscous dissipation of the magnetic fluid was removed by the water. Therefore, the entire test process meets the temperature conditions required by the magnetic fluid.

Figure 11 Magnetic liquid

Figure 12 shows the magnetic fluid sealing device used in the test. The sealing structure was a multistage sealing. The magnetic fluid was injected into the sealing gap of each stage through the hole in the figure. The inner part of the hole was equipped with a thread structure. After the injection of the magnetic fluid was completed, it was sealed with bolts to prevent leakage of the magnetic fluid. According to the data provided by the manufacturer, the maximum sealing pressure of the device is 0.4 MPa, which is substantially greater than the maximum pressure at the sealing gap of the centrifugal pump shaft. Therefore, it satisfies the sealing conditions.

Figure 12 Magnetic liquid sealing device

To monitor the pressure pulsation at the shaft clearance of the centrifugal pump, the pressure fluctuation sensor was placed at the shaft clearance, and the probe size of the pressure fluctuation sensor was much larger than the sealing gap size. Thus, the sealing gap size could not accommodate the sensor. Moreover, the shell of the centrifugal pump was made of cast iron; hence, it could not be welded after cutting, and the pressure sensor was placed at the outlet of the centrifugal pump. The pressure fluctuation at the outlet of the centrifugal pump was monitored in real time and compared with the results of the numerical calculations.

After the test equipment was started and began to run stably, the pressure fluctuation sensor was used to record the pressure fluctuation in four rotation cycles. Figure 13 shows the comparison between the calculated and test values under different flow rates. It can be observed from Figure 13 that at 0.8Q_r, the flow field in the pump was unstable, resulting in a large systematic error in the data acquisition process. Some assumptions of the

ideal state, such as the uniform inlet velocity, no friction on the wall, and volume loss of the balance hole on the impeller were used in the numerical calculation[24]. With an increase in the flow rate, the flow field in the pump became stable. The influence of some uncontrollable factors on the pressure fluctuation began to weaken; therefore, the error between the experimental value and the calculated value was small at a large flow rate. However, in general, the pressure fluctuation curve of the numerical calculation was consistent with that of the experiment, verifying the reliability of the numerical calculation results.

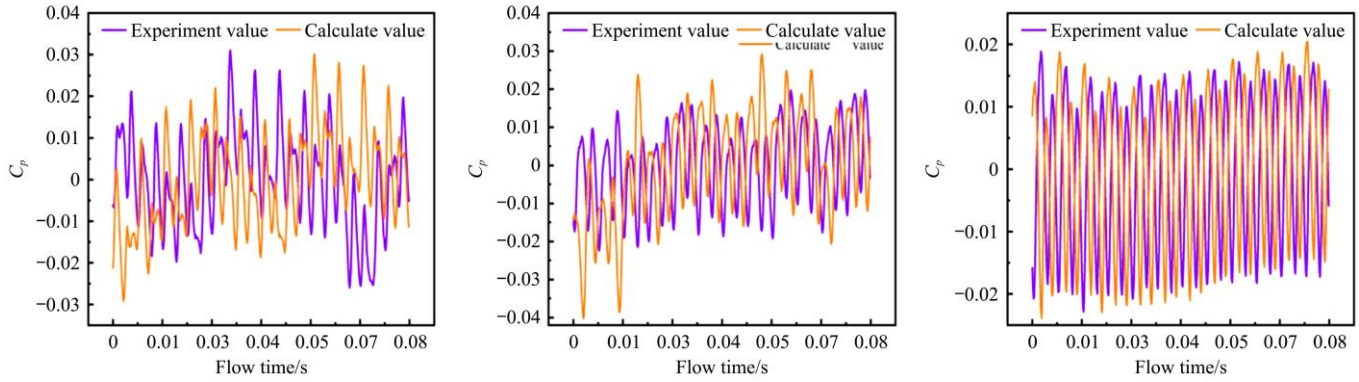

a. $0.8Q_r$ b. $1.0Q_r$ c. $1.2Q_r$

Figure 13 Comparison of calculation results

4 Conclusions

Large pressure fluctuation exists at the sealing interface of the magnetic fluid in the centrifugal pump. Under the same flow rate, the amplitude of the pressure fluctuation decreases slightly from the shaft surface to the bottom of the polar tooth. Under different flow rates, the amplitude of the pressure fluctuation decreases with an increase in the flow rate.

The main causes of pressure fluctuation at the seal interface are the dynamic and static interference between the impeller and volute, flow state of the fluid in the pump, the impact of the liquid in the seal cavity, and water hammer. Cavitation causes flow disorder in the pump, resulting in adverse impact on the magnetic liquid, aggravation of the water hammer, and an increase in the pressure fluctuation amplitude.

When there is no cavitation, the number of reciprocating motions of the magnetic fluid is the same as the number of blades in the period of one revolution of the runner, whereas during cavitation, the frequency of magnetic fluid position movement has no obvious regularity, causing the interface to vibrate, and subsequently leading to severe damage of the stability of the interface.

The results show that there is axial velocity fluctuation at the sealing interface, and the axial velocity fluctuation of the sealing liquid at the bottom end of the polar tooth and the surface of the shaft presents a centrosymmetric law. The erosion effect of the sealing fluid on the sealing interface of the magnetic fluid gradually weakens from the bottom of the pole tooth to the surface of the shaft, and cavitation accelerates the frequency of velocity fluctuation.

The volume fraction of the small bubbles generated by cavitation decreases with an increase in the flow rate at the seal clearance; therefore, the influence of the pressure fluctuation caused by bubble collapse on the stability of the seal interface is weakened under the condition of a large flow rate.

Acknowledgements

The authors would like to acknowledge the support of the National Natural Science Foundation of China (Grant No. 52079118), the Science and Technology Department of Sichuan Province (Grant No. 2020YFH0135), the Open Research Subject of Key Laboratory of Fluid and Power Machinery (Xihua University), Ministry of Education (Grant No. LTDL2021-005), and Project of Science and Technology Department of Sichuan Province, (Grant No. 202573).

Nomenclature

Varibles	Definition
ρ	Fluid medium density, kg/m^3
t	Per unit time
u_x, u_y, u_z	Velocity component of the fluid along the x, y, z axis, m/s
$\boldsymbol{u}$	Fluid velocity, m/s
$\boldsymbol{\tau}$	Viscous force per unit mass of fluid
$\boldsymbol{F}$	Mass force per unit mass of fluid
μ_t	Turbulent viscosity coefficient
μ	Kinematic viscosity of fluid, Pa s
k	Turbulent kinetic energy
ε	Turbulence dissipation rate
c_1^*	c_1 revised
E_{ij}	Shear deformation rate
R_B	Cavity radius, m
v	Kinematic viscosity coefficient
σ	Bubble wall tension, N/m
P_B	Cavitation wall pressure, Pa
p	External pressure of cavitation, Pa
α	Vapor phase volume fraction
ρ_v	The density of vapor phase
R_e	The phase transition rate generated by cavitation
R_c	The phase transition rate of cavitation collapse

[References]

[1] Bao M X, Ni X D, Kang S W. Efficiency analysis of pump-controlled motor system of hydraulic machinery continuously variable transmission for agricultural machinery. InMATEC Web of Conferences, 2020; 319: 03002.

[2] van der Wal K, van Ostayen RA, Lampaert S G. Ferrofluid rotary seal with replenishment system for sealing liquids. Tribol Int. 2020; 150: 106372.

[3] Biao X, Yiping L, Hongjuan R. Review on magneto-rheological fluid and its application. Am J Nanosci Nanotechnol, 2014; 2: 70–74.

[4] Parmar S, Upadhyay RV, Parekh K. Optimization of design parameters affecting the performance of a magnetic fluid rotary seal. Arab J Sci Eng. 2021; 46(3): 2343–2348.
[5] Szczęch M. Magnetic fluid seal critical pressure calculation based on numerical simulations. Simulation, 2020; 96(4): 403–413.
[6] Parmar S, Ramani V, Upadhyay R V, Parekh K. Two stage magnetic fluid vacuum seal for variable radial clearance. Vacuum, 2020; 172: 109087.
[7] He X Z, Miao Y B, Wang L, Li D C. Latest development in sealing of liquid medium with magnetic fluid. China J Vac Sci Technol, 2019; 39(5): 361–366.
[8] Liu T, Cheng Y, Yang Z. Design optimization of seal structure for sealing liquid by magnetic fluids. J Magn Mater, 2005; 289: 411–414.
[9] Qian J G, Yang Z Y. Analysis of liquid-liquid interface stability for magnetic liquid dynamic seal. Fluid Machinery, 2008; 36(12): 21–23, 20. (in Chinese)
[10] Szczęch M. Influence of selected parameters on the reseal instability mechanism in magnetic fluid seals. J Magn, 2019; 24(1): 32–38.
[11] Wang H J. Novel shield between magnetic fluid and sealed liquid: A theoretical and experimental study. Chinese J Vac Sci Technol, 2019; 39(4): 284–287. (in Chinese)
[12] Krakov M S, Zakinyan A R, Zakinyan A A. Instability of the miscible magnetic/non-magnetic fluid interface. J Fluid Mech, 2021; 913(A30): 1–29.
[13] Qian J G, Yang Z Y. Characteristics of a magnetic fluid seal and its motion in an axial variable seal gap. J China Univ Min Technol, 2008; 18(4): 634–636. (in Chinese)
[14] Yang X L, Sun P, Hao F X. Magnetic field finite element analysis of diverging stepped ferrofluid seal with a large gap and two magnetic sources. Int J Appl Electrom, 2020; 63(1): 31–44.
[15] Merklein M, Rösel S. Characterization of a magnetorheological fluid with respect to its suitability for hydroforming. Int J Mater Form, 2010; 3(1): 283–286.
[16] Chalghoum I, Kanfoudi H, Elaoud S, Akrout M, Zgolli R. Numerical modeling of the flow inside a centrifugal pump: Influence of impeller–volute interaction on velocity and pressure fields. Arab J Sci Eng, 2016; 41(11): 4463–4476.
[17] Rakibuzzaman M, Kim K, Suh SH. Numerical and experimental investigation of cavitation flows in a multistage centrifugal pump. J Mech Sci Technol, 2018; 32(3): 1071–1078.
[18] Ye Y H, Zhu X Y, Lai F, Li G J. Application of the semi-analytical cavitation model to flows in a centrifugal pump. Int Commun Heat Mass, 2017; 86: 92–100.
[19] Versteeg H K, Malalasekera W. An introduction to computational fluid dynamics: The finite volume method. Pearson Education, 2007.
[20] Yakhot V, Orszag S A. Renormalization group analysis of turbulence. I. Basic theory. J Sci Comput, 1986; 1(1): 3–51.
[21] Brennen C E. Cavitation and bubble dynamics. Oxford: Oxford University Press; 1995.
[22] Hu B, Zhang Q, Sun Z. Influence of relative position of diffuser leading edge on pressure pulsation in mixed-flow pump. J Irrig Drain Eng, 2021; 39(1): 16–22.
[23] Zhang C, You J, Tai R, Wang X, Liu Y, Cheng Y. CFD simulations of pump-trip runaway process pressure pulsation of a model pump-turbine. J Hydraul Eng, 2020; 39(4): 62–72.
[24] Wang T, Kong F Y, Xia B, Bai Y X, Wang C. The method for determining blade inlet angle of special impeller using in turbine mode of centrifugal pump as turbine. Renew Energy, 2017; 109: 518–528.